PERFORMANCE OF NSLS2 BUTTON BPMs*

W. Cheng#, B. Bacha, B. Kosciuk, O. Singh, S. Krinsky
NSLS-II, Brookhaven National Laboratory, Upton, NY 11973, USA

Abstract

Different types of button BPMs are used in NSLS2 machines. Coaxial vacuum feedthroughs are used to couple the beam induced signal out. The feedthroughs are designed to match the external transmission line and electronics with characteristic impedance of 50 Ohm. Performances of these BPM feedthroughs are presented in this paper.

INTRODUCTION

NSLS2 is an ultra low emittance third generation light source under construction at Brookhaven National Laboratory. It includes 200MeV LINAC, low energy LINAC to Booster (LtB) transfer line, 200MeV to 3GeV Booster ring, high energy Booster to Storage ring (BtS) transfer line and 3GeV Storage Ring. Button type beam position monitors (BPM) are used in these machines to measure the beam position. Table 1 summarizes different button BPMs used at NSLS2.

Table 1: NSLS2 Button BPM Summary

Type	Qty.	Button dia. [mm]	Chamber size
LINAC	5	10.8	Round, R=20mm
LtB Round	5	15	Round, R=20mm
LtB Elliptical	1	15	Elliptical, 90mm*40mm
Booster Arc type	28	15	Elliptical, 41mm*24mm
Booster Straight	8	15	Elliptical, 62mm*22mm
BtS	8	15	Round, R=20mm
Ring LA	180	7	Octagon 76mm*25mm
Ring SA	9	4.7	Rectangular, EPU and DW chambers

There are six large aperture BPMs in one storage ring cell. These BPMs are mounted on the girder using carbon fiber plates. In straight sections where In-Vacuum Undulators (IVU) are installed, the same large aperture BPMs will be installed. Two button assemblies rotate 64 degree to increase vertical sensitivity. Damping wiggler (DW) and EPU straight sections will be equipped with small aperture BPMs. The small aperture BPM has a button size of 4.7mm diameter and the button to button horizontal separation is 10mm. Two button assembly sets will be installed on the chamber rotated by 60 deg, so that the effective horizontal separation is 5mm in order to increase the vertical sensitivity. The damping wiggler chamber size is 60mm*11.5mm. The EPU chamber is 60mm*8mm. All IVU straight section BPMs are installed on high stability supports. There are several special BPMs in the storage ring injection straight which are not included in Table 1. Injection straight BPMs are geometrically shifted horizontally to measure the bumped stored beam or injected beam.

To verify BPM pickup performance, CST [1] simulations were carried out as well as in-situ measurements. The results are presented in the following sections.

FEEDTHROUGH TDR

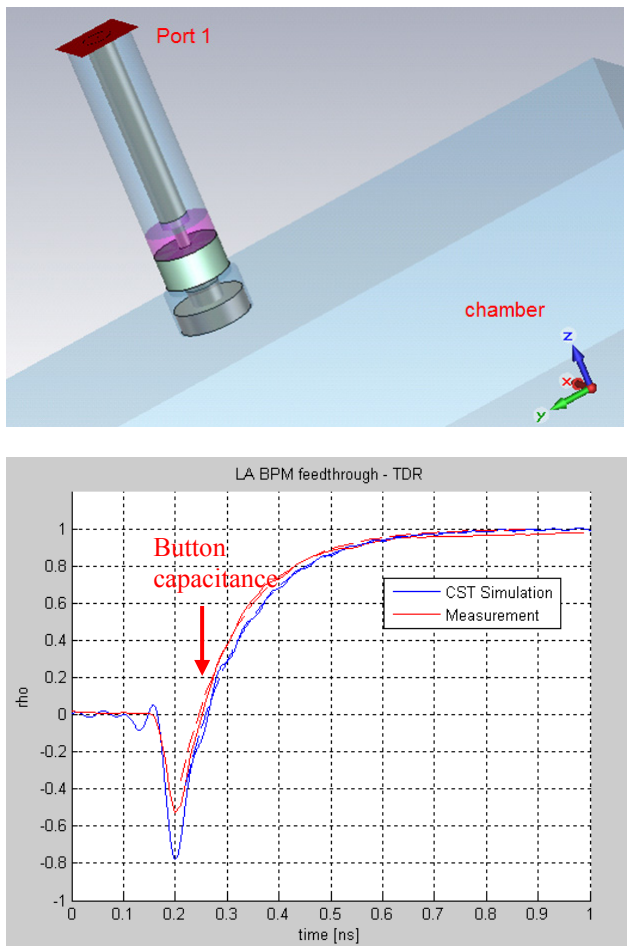

Figure 1: (Top) CST model of NSLS2 storage ring large aperture BPM feedthrough; and (Bottom) TDR simulation result together with real measurement. Fitted results from Eq. (1) were ploted as dashed lines.

*Work supported by DOE contract No: DE-AC02-98CH10886
#chengwx@bnl.gov

ISBN 978-3-95450-127-4

CST Microwave Studio was used to optimize the small aperture BPM feedthrough. To verify the simulation result, we calculated other installed button BPMs as well. Measurements of production feedthrough agree well with the CST simulation results. Fig. 1 shows the example for the storage ring large aperture BPM. The button has 7mm diameter and 2mm thickness. The vacuum glass seal and heat sink are shown as green and pink pieces in the model.

In button BPM TDR curve, reflectivity can be written as:

$$\rho = 1 - e^{-(t-t_0)/\tau}$$
$$\tau = R \cdot C_b \quad (1)$$

Where R is feedthrough characteristic impedance and C_b is button capacitance. Fitting the TDR results to the Eq. (1), button capacitance can be measured. CST simulation TDR curve fitting gives button capacitance of 2.42pF and measurement from 20GHz TDR gives 2.32pF. Measurement and simulation has <5% difference.

TRAPPED MODE

NSLS2 storage ring vacuum chamber has key-hole like geometry. This antechamber structure shifts the chamber cutoff frequency down below the RF frequency where the BPM electronics work at. All 180 large aperture BPMs in the ring, mounted on multipole chambers may detect high order modes, if proper shielding is not installed [2].

Table 2: Comparison of Trapped TE10p Modes Frequency

Mode # p	Equation [MHz]	CST [MHz]	Measure [MHz]
1	960.1	958.4	958.0
2	963.1	961.6	961.0
3	968.0	966.4	966.0
4	974.8	973.6	973.5
5	983.5	982.0	983.0
6	994.1	992.8	994.5
7	1006.5	1004.8	1008.0
8	1020.6	1019.2	
9	1036.3	1034.4	1039.5
10	1053.6	1052.0	1058.0

Resonant mode frequencies of multipole chamber can be written as Eq. (2). Where λ_c is waveguide cutoff wavelength. Lowest modes exist in multipole antechamber structure are TE10p like. NSLS2 multipole chamber has cutoff frequency ~ 432MHz, which is below the RF frequency of 499.68MHz.

$$f_p = \frac{c}{2}\sqrt{\left(\frac{2}{\lambda_c}\right)^2 + \left(\frac{p}{L}\right)^2} \quad (2)$$

To avoid the trapped mode effect on BPM measurements, vacuum compatible BeCu springs were installed in the antechamber gap, which shifts the TE10 cutoff frequency above the RF frequency [2]. For even cell S2 chamber, with RF shielding installed, TE10 cutoff frequency was calculated to be ~ 959.1MHz. Using Eq. (2), possible trapped TE10p modes resonant frequencies can be calculated.

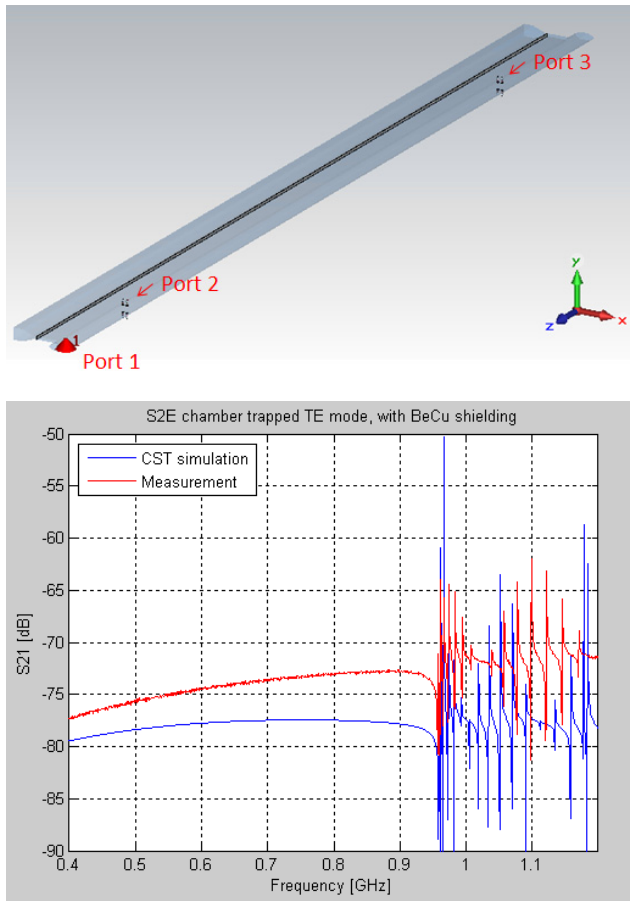

Figure 2: (Top) CST model of NSLS2 even cell S2 multipole chamber with BPMs and shielding installed, excitation ports were defined at BPM buttons and beam chamber. (Bottom) CST simulation result and real chamber measurement.

Using CST frequency domain solver, resonant frequency of trapped modes can be determined from S-parameters between predefined ports. Table 2 compares the TE10p modes frequency from simulation, measurement and Eq (2) calculation, knowing the cutoff frequency from waveguide simulation. With shielding installed, the lowest possible trapped mode will not occur until above 950MHz, which will guarantee BPM electronics free from high order modes. Fig. 2 shows the CST model and S-parameter comparison between simulation and measurement. S21 measured shows the result between two top buttons of the same BPM set. One can see the results agree very well not only with the resonant frequencies, but also with the coupling amplitude between buttons. Measurement and simulation

ISBN 978-3-95450-127-4

S21 amplitude has less than 5dB difference. There are no resonant peaks around 500MHz, which is in favor of detecting electronics.

Due to synchrotron radiation, RF shielding plate cannot extend in the full length of the S6 chamber. The last BPM in each cell will not be protected from the trapped modes. CST simulation and measurement results of S6 chamber are shown in Fig. 3. The measurement was carried out at C22 chamber installed in the ring tunnel. Lowest resonant mode is below 500MHz. The chamber was not under vacuum during the measurement, putting the chamber under vacuum may shift the resonant frequencies. Different production chambers resonant frequencies may shift due to mechanical tolerance.

There are other BPMs installed at positions with no antechamber sections, near the beginning of the cell. This configuration makes sure there are enough useable BPMs for machine commissioning and operation.

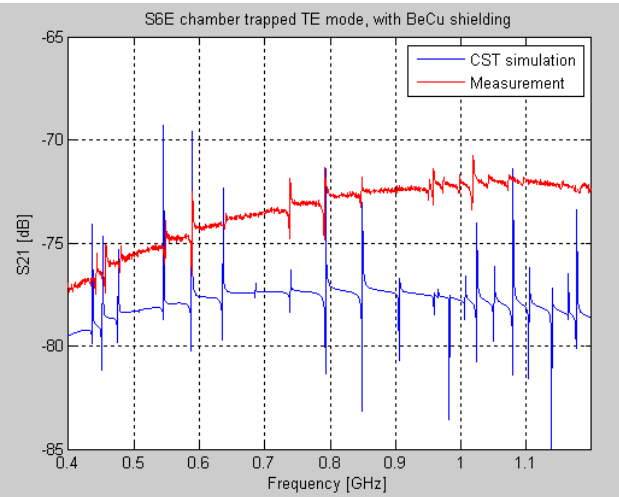

Figure 3: Simulation and measurement results for NSLS2 even cell S6 multipole chamber downstream BPM buttons. RF shielding was installed at upstream part of the chamber but not near the downstream BPM location.

OFFSET MEASUREMENT

Assuming mirror symmetry of the button BPM and housing chamber, offset between the chamber geometry center and BPM electrical center can be measured using a 4-port network analyzer. Description of measurement method can be found in previous paper [3].

All installed BPMs (will) have the offset measured, which will benefit the early stage of commissioning. These measurements also make sure installed button BPMs function as expectation. Ultimately the BPM offset will be measured and corrected with beam based alignment, which determines offset between BPM electrical center relative to the nearby quadruple magnetic center. Fig. 4 presents measurement result for all Booster BPMs, including the arc type and straight section type. Standard deviations of all 36 Booster BPMs' offsets are 126 μm horizontally and 164 μm vertically.

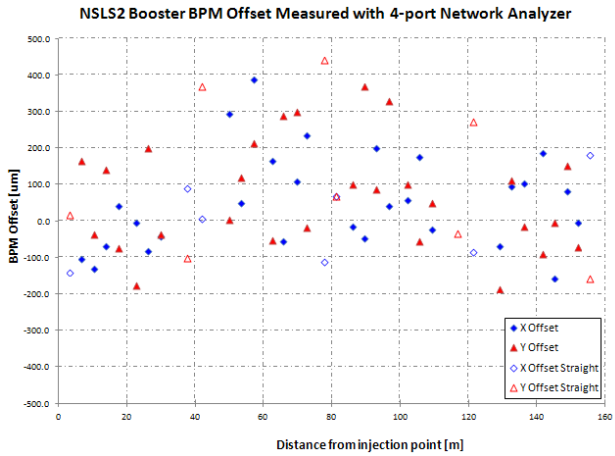

Figure 4: Booster BPM measured offsets.

BPM NONLINEARITY

When the beam has a large offset to the chamber center, the BPM has large nonlinearity on the position read back. As discussed in BIW'2012 paper [3], one or two dimension correlation will be implemented to have read back position as accurate as possible.

BPM four button SUM signals can be very useful for the machine commissioning and operation. Using four-button SUM signal of all 180 BPMs in the storage ring, it's possible to measure the beam lifetime precisely and fast. The DC beam current, filling pattern, electronics gain, and cable loss can all change the measured SUM signal. For a given filling pattern and fixed electronics gain, SUM signal should be determined by the beam current and cable attenuation. Once cable attenuation is known, SUM signal can be useful to measure the beam current. With 180 BPMs distributed along the ring, BPM SUM signal can be especially helpful during commissioning, before the beam stored. One can compare the SUM signal of all BPMs to determine where the beam loss occurred.

Similar to the BPM measured position nonlinearity, when the beam is far from the chamber center, SUM signal has nonlinear effect. With 2D beam offset, one can fit the SUM signal to a polynomial equation. Eq (3) writes the polynomial fit up to 4th order. Due to symmetry, all the odd terms can be neglected.

$$\Sigma_{x,y} = p_{00} + p_{20}x^2 + p_{11}xy + p_{02}y^2 + p_{40}x^4 + p_{31}x^3y + p_{22}x^2y^2 + p_{13}xy^3 + p_{04}y^4 + \ldots \quad (3)$$

As an example of BPM Sum signal nonlinearity, Fig. 5 plots the SUM signal of LINAC BPM at different horizontal/vertical offsets. The value is normalized to central position (0,0) data. There are two mesh plots in

ISBN 978-3-95450-127-4

the drawing. One is calculated raw data and the other layer of mesh plot is fitted result according to Eq. (3). The fitted result agrees well with the raw data, the fitting error is less than 2% in the full range of +/-10mm.

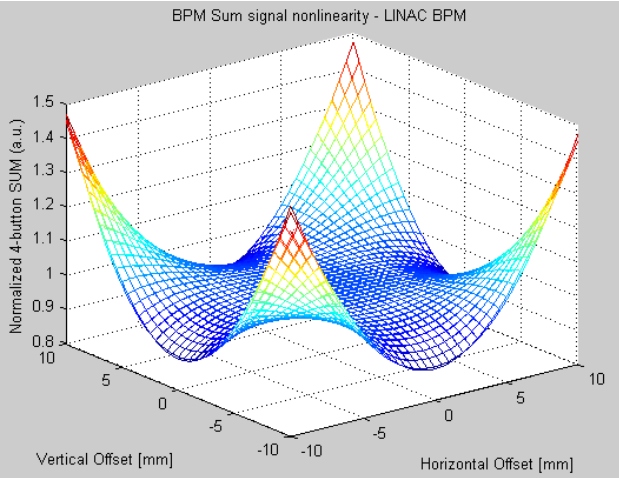

Figure 5: NSLS2 LINAC BPM Sum signal nonlinearity.

Quadratic term Q of four button BPMs can be a useful tool to diagnose the health of buttons, cables and electronics. With small beam offset, where button response is linear, Q-term is close to zero. As the beam moves away from the center, nonlinear effects on Q-term appears. Taylor expanding of button signal to second order, one gets the following relation [4]:

$$Q = c\Delta_x\Delta_y \tag{4}$$

Where $Q = A+C-B-D$, $\Delta_x = A+D-B-C$, $\Delta_y = A+B-C-D$, given A, B, C, D are four buttons starting from top left corner, counting clockwise. c is a constant determined by the BPM chamber geometry.

Calculation result of Q-terms for storage ring large aperture BPM is presented in Fig. 6. Beam positions varied on 10mm*5mm grids. The horizontal grid space was 0.5mm and vertical grid space was 0.25mm. It's clear that Q-term shows nonlinearities even with beam offset as small as ~ mm range. From the plot of Q versus $\Delta_x*\Delta_y$, one can see for NSLS2 storage ring large aperture BPM, more than 2nd order nonlinear terms need to be included. Measurement of this Q-term nonlinearity will be carried out with beam. Using turn-by-turn or slow orbit data from BPM electronics, four feedthrough gain variation (offset) can be measured. The measurement will include the gain variation in the digitizer channels.

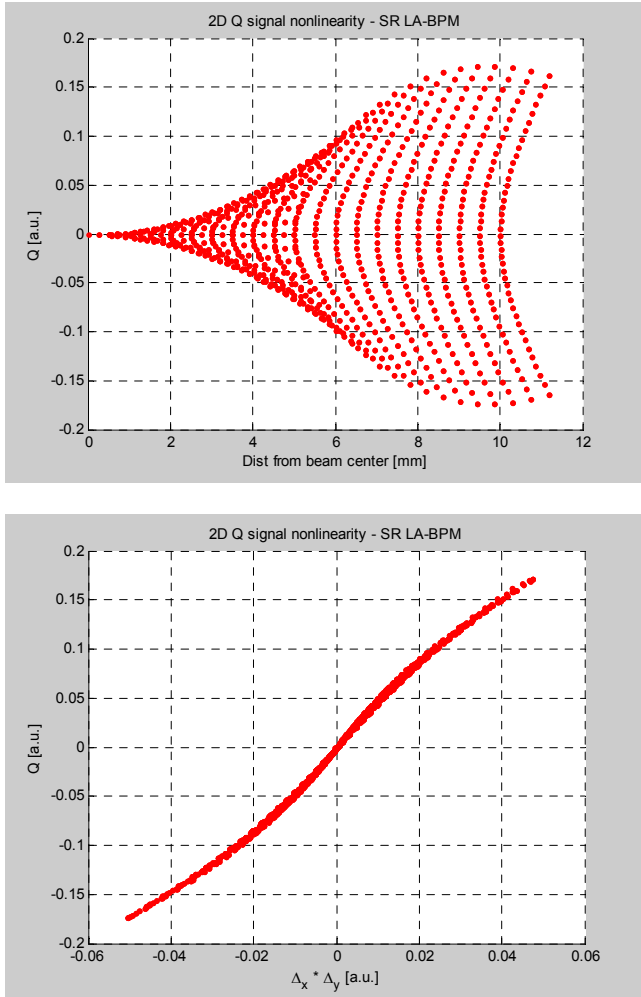

Figure 6: NSLS2 large aperture BPM Q-term nonlinearity. (Top) Q-term vs. distance from chamber center. (Bottom) Q-term vs. Δx*Δy.

SUMMARY

For NSLS2 production BPMs, TDR measurements agree well with CST time domain simulation. Possible trapped mode and its effects to BPM readings have been measured and compared with simulation in agreement with ref [2]. BPM offsets due to four feedthrough gain variation are being measured using network analyzer. Nonlinearity of BPMs, including position, Sum and Q-term have been investigated.

REFERENCES

[1] https://www.cst.com/.
[2] A. Blednykh, et. al., "Rogue Mode Shielding in NSLS2 Multipole Vacuum Chamber", Proc. BIW'2010, http://jacow.org/.
[3] W. Cheng, et. al., "NSLS2 Beam Position Calibration", Proc. BIW'2012, http://jacow.org/.
[4] D. Rubin, et. al., "Beam Based Measurement of Beam Position Monitor Electrode Gains", PRST-AB Vol 13, 092802 (2010)

ISBN 978-3-95450-127-4